Co-design of an event-triggered dynamic output feedback controller for discrete-time LPV systems with constraints

Carla de Souza, Sophie Tarbouriech, Valter J S Leite, Eugênio Castelan

Co-design of an Event-triggered Dynamic Output Feedback Controller for Discrete-time LPV Systems with Constraints[☆]

Carla de Souza[a], Sophie Tarbouriech[b], Valter J. S. Leite[c], Eugênio B. Castelan[d]

[a] *PPGEAS of Universidade Federal de Santa Catarina (UFSC), DAS/CTC/UFSC,* 88040-900*, Florianópolis, SC, Brazil.*
[b] *LAAS-CNRS, Université de Toulouse, CNRS, Toulouse, France.*
[c] *The Department of Mechatronics Engineering,* Campus *Divinópolis — CEFET–MG, R. Álvares Azevedo,* 400*,* 35503-822*, Divinópolis, MG, Brazil.*
[d] *The Department of Automation and Systems, Universidade Federal de Santa Catarina (UFSC), PPGEAS — DAS/CTC/UFSC,* 88040-900*, Florianópolis, SC, Brazil.*

Abstract

This paper investigates an event-triggered control design approach for discrete-time linear parameter-varying (LPV) systems under control constraints. The proposed conditions can simultaneously design a parameter-dependent dynamic output feedback controller and an event generator, ensuring the closed-loop system's regional asymptotic stability. Based on the Lyapunov stability theory, these conditions are given in terms of linear matrix inequalities (LMIs). Moreover, using some proposed optimization procedures, it is possible to minimize the number of sensor transmissions, maximize the estimation of the region of attraction of the origin, and incorporate optimal control criteria into the formulation. Through numerical examples, some comparisons with other approaches in the literature evidence the proposed technique's efficacy.

Keywords: Linear parameter-varying systems. Event-triggered control. Saturation. Dynamic controller. Regional stability.

[☆]This work has been supported by the Brazilian Agencies CAPES under the project Print CAPES-UFSC "Automation 4.0" and CNPq; and by ANR under the project HANDY number 18-CE40-0010.

Email addresses: carla.souza93@hotmail.com (Carla de Souza), sophie.tarbouriech@laas.fr (Sophie Tarbouriech), valter@ieee.org (Valter J. S. Leite), eugenio.castelan@ufsc.br (Eugênio B. Castelan)

1. Introduction

In recent years, event-triggered control (ETC) has gained increasing interest due to its potential to reduce the usage of the communication and computational resources of control systems, which is quite important in communication networks with limited bandwidth and battery-powered wireless devices [1]. The main idea of event-triggering techniques consists of performing control tasks after the occurrence of an event, generated by some well-designed event-triggering mechanism, rather than the elapse of a certain fixed time interval, as in traditional sampled-data control. Consequently, ETC is capable of reducing the control tasks execution while guaranteeing stability and some performance index of the closed-loop system. Moreover, dynamic controllers can perform their tasks with reduced information about the controlled process. Two general categories allow the classification of the existing approaches, namely, emulation based [2] and co-design based approaches [3, 4, 5]. In the context of the emulation-based approach, the design concerns only the controller or the event-triggering condition while the other part is given. In the co-design approach, both parts, the controller and the event-triggering conditions, are simultaneously designed. Note that the co-design may lead to better closed-loop performance and more general and more flexible design conditions. Various ETC strategies can be found in the literature, see, for instance, [6, 7, 8, 9, 10, 11, 12, 13]. However, most previous works handle only linear time-invariant (LTI) and nonlinear systems, without considering both varying parameters and control constraints, such as saturating actuators.

LPV models concern a significant class of linear systems whose dynamics depends on a prior unknown but on-line measurable time-varying parameters [14]. Due to their effectiveness in modeling and control time-varying and nonlinear systems, LPV models have been extensively studied in the literature [15, 14]. However, the simultaneous design of both the event generator and feedback controller, i.e., the co-design, for LPV systems, has been little explored,

mainly in the discrete-time context. In [4], the authors propose an $\mathcal{H}_\infty$ event-triggered control by jointly designing a mixed event-triggering mechanism and state-feedback controllers for discrete-time LPV systems under network-induced delays. A parameter-dependent state-feedback controller and an event generator are co-designed in [16, 17], stabilizing the LPV closed-loop system. Authors in [18] propose a condition for the co-design of a mixed event generator and a parameter-dependent static output-feedback controller for LPV discrete-time systems.

Another important feature when dealing with stability analysis and control design is the presence of saturating actuators. Such a nonlinearity may cause performance degradation or even unstable behavior (see [19] and references therein). Recently, the research on ETC has been extended to consider saturating actuators, both in the continuous-time setting [20, 21, 22, 23, 24, 25, 26] and in the discrete-time one [27, 28, 29, 30, 26]. Authors in [27] propose a procedure to design a state-feedback controller maximizing the region of attraction of a discretized system under saturating actuators for a given event-triggering condition. Another recent approach to minimize the region of attraction concerns discrete-time piecewise affine saturated systems [30]. However, the co-design is not addressed in these cases, which may lead to conservative results. The main difficulty in obtaining co-design methods lies in the nonlinear relations among the optimization variables involved. To overcome such an issue, authors in [28] suggest a cone complementarity linearization algorithm for solving the non-convex optimization problem yielding a method to design both an event-triggering strategy and a state-feedback controller for LTI systems under saturating actuators. In [29, 26], by using similarity transformations, other methods to the simultaneous design of static state-feedback gain and an event-triggering condition are found, ensuring the regional stability of saturated LTI systems. Additionally, [26] also considers the co-design based on a dynamic state stabilizing controller.

Note that the discretization of continuous-time systems under time-varying parameters or variable sampling time may not be straightforward as discussed,

for instance, in [31, 32]. More sophisticated approaches may use sampled-data control handling the process changes between consecutive aperiodic samplings [33, 34]. On the other hand, conventional discretization methods under periodic and small enough sampling may lead to nice discrete-time model-approximations, where the discretization error is negligible [35]. Additionally, as discussed in [36], LPV models obtained from identification methods are usually given in the discrete-time framework [37, 38]. Moreover, for processes that are naturally discrete on time, the discretization issues vanish. Since the focus of the current work relies on the ETM co-design for saturating LPV systems, the discretization procedure is not addressed here. Thus, we assume that the considered system in what follows is an already discretized model with time-varying parameters belonging to a polytopic set. Despite more involving techniques that combine ETM co-design with sampled-data control but without LPV characteristic, see for instance [39, 7], our approach provides useful achievements that overcome other similar conditions from the literature by an enhanced ETM proposal.

The simultaneous design of the event generator and the dynamic output feedback controller remains an open issue for LPV systems under saturating actuators. Therefore, using discrete-time LPV models, the contribution of this paper aims at providing some bricks to address this issue:

1. A convex procedure to design both a parameter-dependent dynamic output-feedback controller with anti-windup action and an event-triggering condition;
2. The provided methodology allows the co-design considering optimization problems aiming at reducing the transmission activity, optimizing a certain level of performance, or maximizing the estimation of the basin of attraction of the origin;
3. The convex methodology can be simplified to design only an event-triggering condition for a given parameter-dependent dynamic output-feedback controller with anti-windup action;

To derive the convex formulation, the Lyapunov theory is used conjointly with S-procedure and the generalized sector condition, yielding a set of linear matrix inequalities (LMIs) that, if feasible, ensures the regional asymptotic stability of the closed-loop system and provides an estimate of the region of attraction of the origin. Furthermore, some optimization problems can be associated with the LMI constraints to deal with triggering activity or the size of the region of closed-loop stability.

The paper is organized as follows. In Section 2, the class of systems under constraints is described and the problem we intended to solve is formally stated. Section 3 is dedicated to preliminary results useful to develop the main conditions. In Section 4, the main results addressing both the emulation and the co-design cases are developed. The optimization problems evoked previously are also derived. In Section 5, numerical examples illustrate the usefulness of the proposed conditions, where simulations and comparisons are established with the related literature. The achieved results suggest our approach leads to fewer updates in the sensor channel. Finally, conclusions are given in Section 6

Notation: The sets of real numbers and non-negative real numbers are denoted by $\mathbb{R}$ and $\mathbb{R}^+$, respectively. The set of integer numbers belonging to the interval from $a \in \mathbb{N}$ to $b \in \mathbb{N}$, $b \geq a$, is denoted by $\mathcal{I}[a, b]$. $\mathbb{R}^{m\times n}$ is the set of matrices with real entries and dimensions $m\times n$. A block-diagonal matrix A with blocks A_1 and A_2 is denoted as $A = \texttt{diag}\{A_1, A_2\}$. The transpose of a vector or matrix A is denoted by $A^\top$ and its ℓ^{th} line is indicated by $A_{(\ell)}$. The matrix $\mathbf{0}$ stands for the null matrix of appropriate dimensions and $\mathbf{I}_n$ corresponds to the identity matrix with dimension $n \times n$. The symbol $\star$ stands for symmetric blocks within a matrix, $\bullet$ represents an element that does not influence on developments.

2. Problem Formulation

Consider the discrete-time saturated LPV system

$$\begin{aligned} x(k+1) &= A(\theta_k)x(k) + B(\theta_k)\mathtt{sat}(u(k)), \\ y(k) &= Cx(k), \end{aligned} \tag{1}$$

where $x(k) \in \mathbb{R}^n$ is the state vector, $y(k) \in \mathbb{R}^p$ is the measurable output, $u(k) \in \mathbb{R}^m$ is the control signal and $\mathtt{sat}(u(k))$ is a symmetric saturation function given by

$$\mathtt{sat}(u_{(\ell)}(k)) = \mathtt{sign}(u_{(\ell)}(k)) \min(|u_{(\ell)}(k)|, \bar{u}_{(\ell)}) \tag{2}$$

where $\bar{u}_{(\ell)} > 0$ denotes the symmetric level relative to the ℓ^{th} control input. The vector of time-varying parameters θ_k, which are assumed measurable and available on-line [14], lies in the unitary simplex with N known vertices defined by

$$\Theta \triangleq \left\{ \sum_{i=1}^{N} \theta_{k(i)} = 1,\ \theta_{k(i)} \geq 0,\ i \in \mathcal{I}[1, N] \right\}. \tag{3}$$

The parameter-dependent matrices $A(\theta_k) \in \mathbb{R}^{n\times n}$ and $B(\theta_k) \in \mathbb{R}^{n\times m}$ can be written in the polytopic form as

$$\begin{bmatrix} A(\theta_k) & B(\theta_k) \end{bmatrix} = \sum_{i=1}^{N} \theta_{k(i)} \begin{bmatrix} A_i & B_i \end{bmatrix}. \tag{4}$$

Note that it is usual to keep the general formulation of (1) to develop general conditions and to focus on the polytopic formulation (4) to obtain tractable numerical conditions. However, due to the controller structure assumed in the sequence, we directly use the polytopic formulation along the text, simplifying the developments.

To regionally stabilize the system (1), we propose the design of the following parameter-dependent dynamic output feedback compensator with anti-windup action:

$$\begin{aligned} x_c(k+1) &= A_c(\theta_k)x_c(k) + B_c(\theta_k)\hat{y}(k) - E_c(\theta_k)\Psi(u(k)), \\ u(k) &= C_c(\theta_k)x_c(k) + D_c(\theta_k)\hat{y}(k), \end{aligned} \tag{5}$$

where $x_c(k) \in \mathbb{R}^n$ is the controller state, $\Psi(u(k)) : \mathbb{R}^m \to \mathbb{R}^m$ is a dead-zone nonlinearity defined by $\Psi(u(k)) = u(k) - \mathtt{sat}(u(k))$, and $\hat{y}(k)$ is the last output measure updated, which was sent by the event-triggering mechanism (ETM). It is worth to say that the matrix $E_c(\theta_k) \in \mathbb{R}^{n\times m}$ is introduced to mitigate the windup effect caused by the saturating actuators. Therefore, the anti-windup acts only when saturation occurs, i.e., whenever $\Psi(u(k)) \neq \mathbf{0}$. Following the standard approach for LPV systems, in this work the information concerning the scheduling parameter is assumed online available for the controller.

In this paper, we are interested by the following ETM:

$$\hat{y}(k) := \begin{cases} y(k), & \text{if } f(\hat{y}, y, u) > 0, \\ \hat{y}(k-1), & \text{otherwise.} \end{cases} \tag{6}$$

where $f(\hat{y}, y, u)$ is the triggering condition defined by

$$f(\hat{y}, y, u) := \|\hat{y}(k-1) - y(k)\|^2_{Q_e} - \|y(k)\|^2_{Q_y} - \|u(k)\|^2_{Q_u} > 0 \tag{7}$$

with symmetric positive definite matrices Q_e, $Q_y \in \mathbb{R}^{p\times p}$ and $Q_u \in \mathbb{R}^{m\times m}$. The interest in such a structure of ETM resides in the use of more information from the closed-loop behavior, beyond the frequent employment of only y and sometimes only u, to decide to transmit or not the signals. Note that, it has already been proved effective in the emulation-based approach as proposed in [40].

By considering the ETM in (6), if (7) is satisfied at instant k, then $\hat{y}(k)$ is update to $y(k)$, because the error $\|\hat{y}(k-1) - y(k)\|^2_{Q_e}$ is too big to guarantee the stability and certain performance index for the closed-loop system. On the other hand, if (7) is not satisfied at instant k, then $\hat{y}(k)$ is not updated, because the error is small enough to guarantee the stability and certain performance index for the closed-loop system. In the latter case, $\hat{y}(k)$ maintains its value from the previous instant, $\hat{y}(k-1)$. The matrices Q_e, Q_y, and Q_u are used here to weigh the terms associated with the triggering condition. The choice of matrices Q_e, Q_y, and Q_u directly impacts the event-triggering policy and, thus, on how much the data transmission rate can be reduced. This work aims

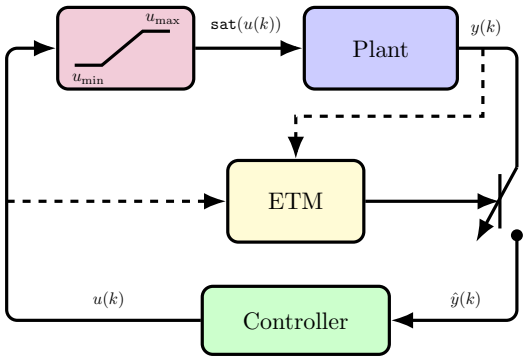

Figure 1: Event-triggered mechanism for the LPV system (1).

to design these matrices conjointly with the ones of the controller (5) to yield a better event-triggered control scheme. The event-triggered control system of interest is depicted in Figure 1.

Additionally, let us consider the following assumption:

Assumption 1. *The matrices of the controller* (5) *are supposed to have the following structure:*

$$\begin{bmatrix} A_c(\theta_k) & B_c(\theta_k) \end{bmatrix} = 0.5 \sum_{i=1}^{N} \sum_{j=i}^{N} (1+\varsigma_{ij}) \theta_{k(i)} \theta_{k(j)} \begin{bmatrix} A_{cij} & B_{cij} \end{bmatrix}, \tag{8}$$

$$\begin{bmatrix} C_c(\theta_k) & D_c(\theta_k) \end{bmatrix} = \sum_{i=1}^{N} \theta_{k(i)} \begin{bmatrix} C_{ci} & D_{ci} \end{bmatrix}, \text{ and } E_c(\theta_k) = \sum_{i=1}^{N} \theta_{k(i)} E_{ci},$$

with $\theta_k \in \Theta$ *and* $\varsigma_{ij} = 1$ *if* $i \neq j$ *and* $\varsigma_{ij} = 0$ *otherwise.*

Note that any dynamic controller given in a polytopic constructive form can be described according to Assumption 1 by using the fact that $\theta_k \in \Theta$ and the following equivalence: $\left(\sum_{i=1}^{N} \theta_{k(i)}\right) \left(\sum_{i=1}^{N} \theta_{k(i)} M_i\right) = 0.5 \sum_{i=1}^{N} \sum_{j=i}^{N} (1 + \varsigma_{ij}) \theta_{k(i)} \theta_{k(j)} M_{ij}$, with $\varsigma_{ij} = 1$ if $i \neq j$ and $\varsigma_{ij} = 0$ otherwise. However, the converse is not always possible because formulation (8) is more general than the polytopic one.

Since there is a saturation in the loop, the system's global stability may not be guaranteed [19]. In this case, the regional (local) stability must be studied and the region of attraction of the origin, denoted $\mathcal{R}_{\mathcal{A}}$, is designed in

terms of the augmented state vector $\xi(k) = \begin{bmatrix} x(k)^\top & x_c(k)^\top \end{bmatrix}^\top \in \mathbb{R}^{2n}$. The region $\mathcal{R}_\mathcal{A}$ is the set of all initial conditions yielding closed-loop trajectories that converge to the origin. As the exact numerical characterization of $\mathcal{R}_\mathcal{A}$ is, generally, a hard task, it is important to determine estimates with a well-fitted analytical representation (see, for example, [19] for more details). By denoting $\mathcal{R}_\mathcal{E}$ the estimate of the region of attraction, then we are interested in computing $\mathcal{R}_\mathcal{E} \subset \mathcal{R}_\mathcal{A}$ as large as possible.

From this, we intend to investigate the following problem:

Problem 1. *For the discrete-time saturated LPV system* (1)*, design both the dynamic output-feedback controller* (5) *under Assumption 1 and the event-triggering condition, $f(\hat{y}, y, u)$, that ensures the regional asymptotic stability of the closed-loop system while reducing the number of data transmissions between the sensor/plant and the controller.*

3. Preliminary Results

The closed-loop system (1)-(5) can be rewritten in a compact form as follows:

$$\begin{aligned} \xi(k+1) &= \mathbb{A}(\theta_k)\xi(k) - \mathbb{B}(\theta_k)\Psi(u(k)) + \mathbb{E}(\theta_k)e(k), \\ u(k) &= \mathbb{K}(\theta_k)\xi(k) + D_c(\theta_k)e(k), \\ y(k) &= \mathbb{C}\xi(k), \end{aligned} \tag{9}$$

where $\xi(k) = \begin{bmatrix} x(k)^\top & x_c(k)^\top \end{bmatrix}^\top \in \mathbb{R}^{2n}$ is the augmented state and $e(k) = \hat{y}(k) - y(k) \in \mathbb{R}^p$ is the output error. The parameter-varying matrices, which also verify from Assumption 1

$$\begin{bmatrix} \mathbb{A}(\theta_k) & \mathbb{E}(\theta_k) \end{bmatrix} = 0.5 \sum_{i=1}^{N} \sum_{j=i}^{N} (1 + \varsigma_{ij}) \theta_{k(i)} \theta_{k(j)} \begin{bmatrix} \mathbb{A}_{ij} & \mathbb{E}_{ij} \end{bmatrix},$$

$$\text{and } \begin{bmatrix} \mathbb{B}(\theta_k) & \mathbb{K}(\theta_k)^\top \end{bmatrix} = \sum_{i=1}^{N} \theta_{k(i)} \begin{bmatrix} \mathbb{B}_i & \mathbb{K}_i^\top \end{bmatrix},$$

with $\theta_k \in \Theta$ and $\varsigma_{ij} = 1$ if $i \neq j$ and $\varsigma_{ij} = 0$ otherwise, are given by

$$\mathbb{A}_{ij} = \begin{bmatrix} A_i + A_j + (B_i D_{cj} + B_j D_{ci})C & B_i C_{cj} + B_j C_{ci} \\ B_{cij} C & A_{cij} \end{bmatrix}, \ \mathbb{B}_i = \begin{bmatrix} B_i \\ E_{ci} \end{bmatrix}$$

$$\mathbb{E}_{ij} = \begin{bmatrix} B_i D_{cj} + B_j D_{ci} \\ B_{cij} \end{bmatrix}, \ \mathbb{K}_i = \begin{bmatrix} D_{ci} C & C_{ci} \end{bmatrix}, \text{ and } \mathbb{C} = \begin{bmatrix} C & \mathbf{0} \end{bmatrix}.$$

If (7) is satisfied at instant k, then we have from (6) that $e(k) = \hat{y}(k) - y(k) = y(k) - y(k) = 0$, and if (7) is not satisfied at instant k, then we have from (6) that $e(k) = \hat{y}(k) - y(k) = \hat{y}(k-1) - y(k)$. So, the following inequality

$$\|e(k)\|^2_{Q_e} \leq \|y(k)\|^2_{Q_y} + \|u(k)\|^2_{Q_u} \tag{10}$$

is always satisfied.

To investigate the regional asymptotic stability of the closed-loop system (9), we use the Lyapunov theory with the following Lyapunov candidate function

$$V(k) = \xi(k)^\top P^{-1}(\theta_k)\xi(k), \tag{11}$$

where $P(\theta_k) = \sum_{i=1}^{N} \theta_{k(i)} P_i$, with $\mathbf{0} < P_i = P_i^\top \in \mathbb{R}^{2n \times 2n}$ and $\theta_k \in \Theta$. If (11) is a Lyapunov function, then the estimate of the region of attraction of the origin for the closed-loop system is computed as

$$\mathcal{R}_{\mathcal{E}} = \bigcap_{\theta_k \in \Theta} \mathcal{E}(P(\theta_k)^{-1}, 1) = \bigcap_{i \in \mathcal{I}[1,N]} \mathcal{E}(P_i^{-1}, 1) \tag{12}$$

with

$$\mathcal{E}(P_i^{-1}, 1) = \{\xi(k) \in \mathbb{R}^{2n} : \xi(k)^\top P_i^{-1} \xi(k) \leq 1, \forall i \in \mathcal{I}[1, N]\}. \tag{13}$$

Moreover, to deal with the actuator saturation, we use the following lemma directly derived from [19].

Lemma 1. *Consider a matrix $G(\theta_k) = \sum_{i=1}^{N} \theta_{k(i)} G_i$ with $G_i \in \mathbb{R}^{m \times 2n}$ for all $\mathcal{I}[1, N]$ and $\theta_k \in \Theta$. If $\xi(k)$ belongs to the set $\mathcal{S}(\bar{u})$ defined by*

$$\mathcal{S}(\bar{u}) \triangleq \{\xi(k) \in \mathbb{R}^{2n} : |G(\theta_k)\xi(k)| \leq \bar{u}\}, \tag{14}$$

then the nonlinearity $\Psi(u(k))$ satisfies the following inequality:

$$\Psi^\top(u(k)) M (\Psi(u(k)) - (\mathbb{K}(\theta_k) - G(\theta_k))\xi(k) - D_c(\theta_k)e(k)) \leq 0, \tag{15}$$

or equivalently,

$$\Psi^\top(u(k))M(-\mathtt{sat}(u(k)) + G(\theta_k)\xi(k)) \leq 0, \tag{16}$$

for any diagonal positive definite matrix $M \in \mathbb{R}^{m\times m}$.

4. Main Results

In this section, the emulation case is first considered, consisting of designing the event-triggering rule $f(\hat{y}, y, u)$ with a given dynamic output-feedback controller (5). This result is then extended to design both the event-triggering rule $f(\hat{y}, y, u)$ and the dynamic output-feedback controller. Finally, three optimization procedures are proposed to match different control objectives.

4.1. Emulation case

The following result focuses on designing the event-triggering rule $f(\hat{y}, y, u)$ when the dynamic controller is assumed given.

Theorem 1. *Given the matrices* A_{cij}, B_{cij}, C_{ci}, D_{ci}, *and* E_{ci} *of the compensator in* (5), *consider that there exist symmetric positive definite matrices* $P_i \in \mathbb{R}^{2n\times 2n}$, Q_e, $\hat{Q}_y \in \mathbb{R}^{p\times p}$, *and* $\hat{Q}_u \in \mathbb{R}^{m\times m}$, *positive definite diagonal matrix* $S \in \mathbb{R}^{m\times m}$, *and matrices* $U \in \mathbb{R}^{2n\times 2n}$ *and* $H_i \in \mathbb{R}^{m\times 2n}$, *with* $i \in \mathcal{I}[1, N]$, *satisfying*

$$\underbrace{\left[\begin{array}{c|c|c|c|c|c} U + U^\top & \star & \star & \star & \star & \star \\ -\frac{1}{2}(P_i + P_j) & & & & & \\ \hline \mathbf{0} & Q_e & \star & \star & \star & \star \\ \hline \frac{1}{2}(H_i + H_j & -\frac{1}{2}(D_{ci} + D_{cj}) & 2S & \star & \star & \star \\ -\mathbb{K}_i U - \mathbb{K}_j U) & & & & & \\ \hline \frac{1}{2}\mathbb{A}_{ij}U & \frac{1}{2}\mathbb{E}_{ij} & -\frac{1}{2}(\mathbb{B}_i + \mathbb{B}_j)S & P_r & \star & \star \\ \hline \mathbb{C}U & \mathbf{0} & \mathbf{0} & \mathbf{0} & \hat{Q}_y & \star \\ \hline \frac{1}{2}(\mathbb{K}_i + \mathbb{K}_j)U & \frac{1}{2}(D_{ci} + D_{cj}) & \mathbf{0} & \mathbf{0} & \mathbf{0} & \hat{Q}_u \end{array}\right]}_{\mathcal{M}_{rij,1}} > \mathbf{0},$$

$$r, i \in \mathcal{I}[1, N];\ j \in \mathcal{I}[i, N]; \tag{17}$$

and

$$\begin{bmatrix} U + U^\top - P_i & \star \\ H_{i(\ell)} & \bar{u}_{(\ell)}{}^2 \end{bmatrix} > \mathbf{0}, \\ i \in \mathcal{I}[1, N], \ell \in \mathcal{I}[1, m]. \tag{18}$$

Then, the closed-loop system (9) subject to the event-triggering condition (6)-(7) with matrices Q_e, $Q_y = \hat{Q}_y^{-1}$, and $Q_u = \hat{Q}_u^{-1}$ is regionally asymptotically stable and has a reduced number of data transmissions between the sensor/plant and the controller. Moreover, the region $\mathcal{R}_\mathcal{E}$, defined in (12)-(13), is an estimate of the region of attraction of the origin for the closed-loop system.

Proof 1. *The proof of Theorem 1 is presented in Appendix A.*

4.2. Co-design

Before presenting the conditions for the co-design of the event-triggering rule $f(\hat{y}, y, u)$ and the dynamic output-feedback controller (5), we introduce some matrices that are useful in the development of the results. Based on the approach proposed by [41], let us define the following matrices

$$U = \begin{bmatrix} X & \bullet \\ Z & \bullet \end{bmatrix}, \quad U^{-1} = \begin{bmatrix} Y & \bullet \\ W & \bullet \end{bmatrix}, \text{ and } \Omega = \begin{bmatrix} Y & \mathbf{I}_n \\ W & \mathbf{0} \end{bmatrix}. \tag{19}$$

with X, Y, W and $Z \in \mathbb{R}^{n \times n}$.

Therefore, we have

$$U\Omega = \begin{bmatrix} \mathbf{I}_n & X \\ \mathbf{0} & Z \end{bmatrix} \text{ and } \hat{U} = \Omega^\top U \Omega = \begin{bmatrix} Y^\top & F^\top \\ \mathbf{I}_n & X \end{bmatrix}, \tag{20}$$

where, by construction

$$F^\top = Y^\top X + W^\top Z. \tag{21}$$

Furthermore, using the partitioning

$$P_i = \begin{bmatrix} P_{i11} & P_{i12} \\ \star & P_{i22} \end{bmatrix},$$

we obtain

$$\hat{P}_i = \Omega^\top P_i \Omega = \begin{bmatrix} \hat{P}_{i11} & \hat{P}_{i12} \\ \star & \hat{P}_{i22} \end{bmatrix}, \tag{22}$$

with $\hat{P}_{i11} = Y^\top P_{i11} Y + W^\top P_{i12}^\top Y + Y^\top P_{i12} W + W^\top P_{i22} W$, $\hat{P}_{i12} = Y^\top P_{i11} + W^\top P_{i12}^\top$ and $\hat{P}_{i22} = P_{i11}$.

Theorem 2. *Consider that there exist symmetric positive definite matrices $\hat{P}_i \in \mathbb{R}^{2n\times 2n}$, Q_e, $\hat{Q}_y \in \mathbb{R}^{p\times p}$ and $\hat{Q}_u \in \mathbb{R}^{m\times m}$, a positive definite diagonal matrix $S \in \mathbb{R}^{m\times m}$ and matrices H_i, X, Y, F, $\hat{A}_{cij}$, $\hat{B}_{cij}$, $\hat{C}_{ci}$, $\hat{D}_{ci}$, and $\hat{E}_{ci}$ of appropriate dimensions, with $i \in \mathcal{I}[1,N]$ and $j \in \mathcal{I}[i,N]$, such that the two following LMIs conditions are feasible.*

$$\underbrace{\left[\begin{array}{c|c|c|c|c|c} \hat{U}+\hat{U}^\top \\ -\frac{1}{2}(\hat{P}_i+\hat{P}_j) & \star & \star & \star & \star & \star \\ \hline \mathbf{0} & Q_e & \star & \star & \star & \star \\ \hline \frac{1}{2}(H_i+H_j-\Pi_{1ij}) & -\frac{1}{2}(\hat{D}_{ci}+\hat{D}_{cj}) & 2S & \star & \star & \star \\ \hline \frac{1}{2}\Pi_{2ij} & \frac{1}{2}\Pi_{3ij} & \frac{1}{2}\Pi_{4ij} & \hat{P}_r & \star & \star \\ \hline C \quad CX & \mathbf{0} & \mathbf{0} & \mathbf{0} & \hat{Q}_y & \star \\ \hline \frac{1}{2}\Pi_{1ij} & \frac{1}{2}(\hat{D}_{ci}+\hat{D}_{cj}) & \mathbf{0} & \mathbf{0} & \mathbf{0} & \hat{Q}_u \end{array}\right]}_{\mathcal{M}_{rij,2}} > \mathbf{0}, \tag{23}$$

$$r, i \in \mathcal{I}[1,N], j \in \mathcal{I}[i,N];$$

and

$$\begin{bmatrix} \hat{U}+\hat{U}^\top - \hat{P}_i & \star \\ H_{i(\ell)} & \bar{u}_{(\ell)}^2 \end{bmatrix} > \mathbf{0}, \tag{24}$$

$$i \in \mathcal{I}[1,N], \ell \in \mathcal{I}[1,m];$$

with

$$\Pi_{1ij} = \begin{bmatrix} (\hat{D}_{ci} + \hat{D}_{cj})C & \hat{C}_{ci} + \hat{C}_{cj} \end{bmatrix},$$

$$\Pi_{2ij} = \begin{bmatrix} Y^\top(A_i + A_j) + \hat{B}_{cij}C & \hat{A}_{cij} \\ A_i + A_j + (B_i\hat{D}_{cj} + B_j\hat{D}_{ci})C & (A_i + A_j)X + (B_i\hat{C}_{cj} + B_j\hat{C}_{ci}) \end{bmatrix},$$

$$\Pi_{3ij} = \begin{bmatrix} \hat{B}_{cij} \\ B_i\hat{D}_{cj} + B_j\hat{D}_{ci} \end{bmatrix}, \Pi_{4ij} = \begin{bmatrix} -(\hat{E}_{ci} + \hat{E}_{cj}) \\ -(B_j + B_i)S \end{bmatrix}, \text{ and } \hat{U} = \begin{bmatrix} Y^\top & F^\top \\ \mathbf{I}_n & X \end{bmatrix}.$$

Then, by choosing non-singular matrices W and Z such that (21) holds, we have that the saturated LPV system (1) *in closed loop with the dynamic output-feedback compensator* (5) *defined by*

$$\begin{aligned} D_{ci} &= \hat{D}_{ci}, \\ C_{ci} &= (\hat{C}_{ci} - D_{ci}CX)Z^{-1}, \\ B_{cij} &= (W^{-1})^\top(\hat{B}_{cij} - Y^\top(B_iD_{cj} + B_jD_{ci}), \\ A_{cij} &= (W^{-1})^\top(\hat{A}_{cij} - Y^\top(A_i + A_j + (B_iD_{cj} + B_jD_{ci})C)X - W^\top B_{cij}CX \\ &\quad - Y^\top(B_iC_{cj} + B_jC_{ci})Z)Z^{-1}, \\ E_{ci} &= (W^{-1})^\top(\hat{E}_{ci}S^{-1} - Y^\top B_i), \end{aligned} \tag{25}$$

subject to the event-triggering condition (6)-(7) with matrices Q_e, $Q_y = \hat{Q}_y^{-1}$, and $Q_u = \hat{Q}_u^{-1}$ is regionally asymptotically stable and has a reduced number of data transmissions between the sensor/plant and the controller. Moreover, the region $\mathcal{R}_\mathcal{E}$, defined in (12)-(13), is an estimate of the region of attraction of the origin for the closed-loop system.

Proof 2. *The proof of Theorem 2 is presented in Appendix B.*

For more information on how to choose matrices Z and W see, for instance, Remark 2.8 in [19]. Also observe that Theorem 2 can also be used to design a dynamic output-feedback controller when the event-triggering mechanism (6)-(7) is fixed, i.e., when the matrices Q_e, Q_y and Q_u are fixed.

Remark 1. *Theorems 1 and 2 can be adapted to treat both precisely known and non-saturating systems. In the first case (known system), it is necessary to set*

$r = i = j = 1$, *which leads to fixed matrices. In this case, the dynamic and input matrices of the controller,* A_c *and* B_c*, are recovered by* (8) *as* $A_c = 0.5A_{c11}$ *and* $B_c = 0.5B_{c11}$*, with* A_{c11} *and* B_{c11} *computed as in* (25)*. In the second case (no saturation), one has to impose:* i) *the line and column* 3 *are deleted in the LMIs* (17) *and* (23)*, and* ii) *the LMIs* (18) *and* (24) *are discarded.*

Remark 2. *Particular cases of the event-triggering condition* (7) *can be considered by imposing certain structures on the matrices* Q_e*,* Q_y*, and* Q_u*. A simple one is to set* i) $Q_e = \mathbf{I}_p$*,* $Q_y = \sigma_y \mathbf{I}_p$*, and* $Q_u = \sigma_u \mathbf{I}_p$*. Its simplicity however can generate more conservative results. To add more degrees of freedom to the design, we can also assume less restrictive forms such as* ii) $Q_e = \mathbf{I}_p$*,* $Q_y = \mathtt{diag}\{\sigma_{y1}, \sigma_{y2}, \ldots, \sigma_{yn}\}$*, and* $Q_u = \mathtt{diag}\{\sigma_{u1}, \sigma_{u2}, \ldots, \sigma_{un}\}$*. Similar versions of both cases are considered, for example, in [42], where the event-triggering condition is based on a state observer and the control signal is not taken into account. By assuming that the event-triggering condition is given, an interesting choice that allows to evaluate the influence of the output and the control signal on the condition, is to set* iii) $Q_e = \mathbf{I}_p$*,* $Q_y = \sigma^2 \mu \mathbf{I}_p$*, and* $Q_u = \sigma^2(1-\mu)\mathbf{I}_m$ *with* $\mu \in \mathcal{I}[0,1]$*, allowing the designer to adjust the weight of the control and output signals by tuning the parameter* μ*. Because the ETM parameters are given, the S-procedure can be applied to include the event-triggering condition. Such a case, considered in [43], allows to include a positive constant* κ *multiplying the right-hand side of* (A.4) *(see the proof of Theorem 1 in Appendix A), being a degree of freedom in the optimization. On the other hand, the conditions are no longer LMIs, thus requiring a linear search on* κ *values.*

4.3. Optimization procedures

In the sequel, we address three objectives to improve the closed-loop operation. We introduce convex procedures to optimize these objectives by using the conditions stated in Theorems 1 and 2. The first one concerns the design of the event-triggering condition to minimize the data transmission rate. The second

one consists of minimizing a functional cost, ensuring the improvement of the closed-loop system's performance in an optimal sense. The last one refers to the maximization of the estimated attraction region of the closed-loop system.

4.3.1. Minimization of the update rate

In this case, the objective is to design both the dynamic controller (5) and the event-triggering condition $f(\hat{y}, y, u)$ to minimize the transmission activity over the network, i.e., minimize the number of of output signal updates. Regarding the inequality (10), we can reduce the update rate by reducing the weight on the error measure, i.e., by choosing Q_e to shrink $\|\hat{y}(k) - y(k)\|_{Q_e}$ compared with the magnitude of the norm-sum of the output, $y(k)$, and control, $u(k)$, signals. Then, an intuitive method to reduce the transmission activity is to minimize the trace of Q_e whereas the trace of Q_u and Q_y are maximized, or equivalently

$$\mathcal{O}_1 : \begin{cases} \min & \mathtt{tr}(Q_e + \hat{Q}_y) + \mathtt{tr}(\hat{Q}_u) \\ \text{subject to} & \begin{cases} (17) \text{ and } (18) \\ \quad \text{or} \\ (23) \text{ and } (24) \end{cases} \end{cases} \tag{26}$$

with $\hat{Q}_y = Q_y^{-1}$ and $\hat{Q}_u = Q_u^{-1}$. Let us stress that the data transmission activity is indirectly reduced thanks to the optimization procedure $\mathcal{O}_1$, which showed up to be effective in most of the tests performed by the authors. Whenever it is not the case, taking into account the generality of the objective function it might be interesting to impose additional constraints on some of the matrices, as done in [40]. Moreover, since the matrices Q_e, Q_y and Q_u are definite positives, the optimal value of the optimization procedure $\mathcal{O}_1$ is ensured to be bounded.

Other alternatives, such as weighting the matrices and replacing the objective function in (26) by $\mathtt{tr}(\alpha_e Q_e + \alpha_y \hat{Q}_y) + \alpha_u \mathtt{tr}(\hat{Q}_u)$ would be possible. Such kind of variation is not investigated here.

4.3.2. Optimal Linear Quadratic Cost

To ensure a certain level of control performance for the closed-loop system (9) under the event-triggering mechanism (6)-(7), we associate with the closed-loop system, the following linear quadratic cost function:

$$J_\infty = \sum_{k=0}^{\infty} J(k) = \sum_{k=0}^{\infty} x(k)^\top Q x(k) + u(k)^\top R u(k), \tag{27}$$

where $Q \in \mathbb{R}^{n\times n}$ and $R \in \mathbb{R}^{m\times m}$ are symmetric and positive definite matrices. Such performance requirement associated with the previous requirements of the closed-loop system yields

$$\begin{aligned}\Delta V(k) - 2\Psi(u(k))^\top M(\Psi(u(k)) - (\mathbb{K}(\theta_k) - G(\theta_k))\xi(k) - D_c(\theta_k)e(k)) \\ - e(k)^\top Q_e e(k) + y(k)^\top Q_y y(k) + u(k)^\top Q_u u(k) < -J(k) \leq 0.\end{aligned} \tag{28}$$

Based on this assumption, we can reformulate the conditions in Theorems 1 and 2, ensuring both the regional asymptotic stability of the closed-loop system and a guaranteed cost J_∞ for the closed-loop system. The proof is omitted because it follows the same steps of the proofs presented in Appendix A and Appendix B, but considering (28). In such a case, LMIs (17) and (23) become

$$\left[\begin{array}{ccccc|c} \multicolumn{5}{c|}{\mathcal{M}_{rij,\times}} & \star \\ \hline \frac{1}{2}\Pi_{5ij} & \frac{1}{2}\Pi_{6ij} & \mathbf{0} & \mathbf{0} & \mathbf{0} & \mathbf{I}_{n+m} \end{array}\right] > \mathbf{0}, \tag{29}$$

where, for Theorem 1, $\mathcal{M}_{rij,\times} = \mathcal{M}_{rij,1}$, the matrix of the left-hand side of relation (17), and Π_{5ij} and Π_{6ij} are given by

$$\Pi_{5ij} = \hat{Q}^{1/2}\begin{bmatrix} 2\mathbb{I} \\ \mathbb{K}_i + \mathbb{K}_j \end{bmatrix} U \text{ and } \Pi_{6ij} = \hat{Q}^{1/2}\begin{bmatrix} \mathbf{0} \\ D_{ci} + D_{cj} \end{bmatrix}; \tag{30}$$

with $\mathbb{I} = \begin{bmatrix}\mathbf{I}_n & \mathbf{0}\end{bmatrix}$, and, for Theorem 2, $\mathcal{M}_{rij,\times} = \mathcal{M}_{rij,2}$, the matrix of the left-hand side of relation (23), and Π_{5ij} and Π_{6ij} are given by

$$\Pi_{5ij} = \hat{Q}^{1/2}\begin{bmatrix} 2\mathbf{I}_n & 2X \\ (\hat{D}_{ci} + \hat{D}_{cj})C & (\hat{C}_{ci} + \hat{C}_{cj}) \end{bmatrix} \text{ and } \Pi_{6ij} = \hat{Q}^{1/2}\begin{bmatrix} \mathbf{0} \\ \hat{D}_{ci} + \hat{D}_{cj} \end{bmatrix}. \tag{31}$$

In both cases, we have $\hat{Q} = \texttt{diag}\{Q, R\}$.

Moreover, by summing (28) up from $k = 0$ to $k = \infty$, we have that $J_\infty < \xi(0)^\top P^{-1}(\theta_0)\xi(0)$. Thus the upper-bound of the cost function J_∞ is related to the Lyapunov matrix $P^{-1}(\theta_0)$ and to the initial state $\xi(0)$. Also, from (22) one gets $P^{-1} = \Omega\hat{P}^{-1}\Omega^\top$, and by considering $x_c(0) = \mathbf{0}$, we have that

$$J_\infty < x(0)^\top \begin{bmatrix} Y & \mathbf{I} \end{bmatrix} \hat{P}^{-1}(\theta_0) \begin{bmatrix} Y & \mathbf{I} \end{bmatrix}^\top x(0). \tag{32}$$

Therefore, to ensure an optimal cost for the closed-loop system, we can minimize a scalar $\eta \geq 0$ such that

$$\eta - \mathtt{tr}(P^{-1}(\theta_0)) \geq 0, \tag{33}$$

or, still,

$$\eta - \mathtt{tr}\left(\begin{bmatrix} Y & \mathbf{I} \end{bmatrix} \hat{P}^{-1}(\theta_0) \begin{bmatrix} Y & \mathbf{I} \end{bmatrix}^\top \right) \geq 0. \tag{34}$$

With the aid of the Schur complement, the costs conditions (33) and (34) are expressed in the form of LMIs as follows:

$$\left[\begin{array}{c|c} \eta\mathbf{I}_{2n} & \mathbf{I}_{2n} \\ \hline \star & P(\theta_0) \end{array}\right] \geq \mathbf{0}, \tag{35a}$$

$$\left[\begin{array}{c|cc} \eta\mathbf{I}_{n} & Y & \mathbf{I}_{n} \\ \hline \star & \multicolumn{2}{c}{\hat{P}(\theta_0)} \end{array}\right] \geq \mathbf{0}, \tag{35b}$$

respectively. Note that the LMIs (35a) and (35b) should be satisfied only for $P(\theta_0) = \sum_{i=1}^{N} \theta_{0(i)} P_i$ and $\hat{P}(\theta_0) = \sum_{i=1}^{N} \theta_{0(i)} \hat{P}_i$, respectively, with θ_0 known. However, if θ_0 is not known *a priori*, we have to check the conditions for all P_i and $\hat{P}_i$ with $i \in \mathcal{I}[1, N]$ to ensure they are satisfied for any θ_0.

Therefore, the optimization procedure can be summarized as:

$$\mathcal{O}_2 : \begin{cases} \min & \eta \\ \\ \text{subject to} & \begin{cases} (29) \text{ with } (30), (18) \text{ and } (35a), \\ \qquad\qquad \text{or} \\ (29) \text{ with } (31), (24) \text{ and } (35b). \end{cases} \end{cases} \tag{36}$$

4.3.3. Maximization of the estimation of the region of attraction $\mathcal{R}_{\mathcal{E}}$

The objective here is to design the ETM or the ETM and the controller such that the estimate of the region of attraction is as large as possible. One way to do that is to maximize the volume of an ellipsoidal $\mathcal{E}(P_0, 1)$, defined in the same way as in (13), such that $\mathcal{E}(P_0, 1) \subseteq \mathcal{R}_{\mathcal{E}}$, which can be ensured by

$$\begin{bmatrix} P_0 & \mathbf{I}_{2n} \\ \star & P_i \end{bmatrix} \geq \mathbf{0}, \text{ or still} \tag{37a}$$

$$\begin{bmatrix} P_0 & \Omega \\ \star & \hat{P}_i \end{bmatrix} \geq \mathbf{0}, \tag{37b}$$

with Ω given in (19) and for all $i \in \mathcal{I}[1, N]$. However, the LMI (37b) is non-convex due to the presence of W in Ω. To overcome such an issue, let us consider the partitioning $P_0 = \begin{bmatrix} P_{011} & P_{012} \\ \star & P_{022} \end{bmatrix}$ and $x_c(0) = \mathbf{0}$, which allows us to dismiss the rows concerning the position of W in Ω. With that, the inequality (37b) can be rewritten as

$$\left[\begin{array}{c|cc} P_{011} & Y & \mathbf{I}_n \\ \hline \star & \multicolumn{2}{c}{\hat{P}_i} \end{array}\right] \geq \mathbf{0}, \tag{38}$$

for all $i \in \mathcal{I}[1, N]$. Thus, we have the following optimization procedure

$$\mathcal{O}_3 : \begin{cases} \min & \mathtt{tr}(P_0) \\ \text{subject to} & (17), (18), (37a), \end{cases} \text{ or } \begin{cases} \min & \mathtt{tr}(P_{011}) \\ \text{subject to} & (23), (24), (38). \end{cases} \tag{39}$$

Remark 3. *It is possible to combine the optimization procedures described in this section to have a trade-off between reducing the number of updates and increasing the estimate of the region of attraction of the origin for the closed-loop system. In such a case, the objective function could be the weighted sum of each of the objective functions.*

5. Simulation results

In this section, we present numerical examples and simulations to validate our strategy and show its effectiveness. We apply the different optimization

procedures given in Section 4.3 and compare the results with similar methods found in the literature. We explore both the LPV and the LTI cases, with and without saturating actuators.

5.1. System under saturating actuators

Consider the system (1) with matrices satisfying (3) and (4) described by

$$\begin{aligned} A_1 &= \begin{bmatrix} 0.8040 & 0.0401 \\ 0.1602 & 0.8040 \end{bmatrix}, \; A_2 = \begin{bmatrix} 1.2060 & 0.0601 \\ 0.2404 & 1.2060 \end{bmatrix}, \\ B_1 &= \begin{bmatrix} 0.0401 \\ 0.0040 \end{bmatrix}, \; B_2 = \begin{bmatrix} 0.0601 \\ 0.0060 \end{bmatrix}, \; C = \begin{bmatrix} 1 & 1 \end{bmatrix}, \end{aligned} \tag{40}$$

and a saturating actuator with symmetric saturation limits $\bar{u} = 5$. Our objective is to make the co-design for this system, i.e., we want to design the dynamic controller (5) and the ETM (6)-(7), simultaneously, so that the update rate is minimized.

By using the optimization procedure $\mathcal{O}_1$ given in (26) with conditions of Theorem 2, we got the ETM with $Q_e = 18.2721$, $Q_y = 0.5878$, and $Q_u = 0.0626$. Figure 2 shows the achieved estimate of the region of attraction, $\mathcal{R}_\mathcal{E}$, in the space of the system's state, where the cut of $\mathcal{R}_\mathcal{E}$ is marked with green dots ($x_c(0) = \mathbf{0}$), and the projection of $\mathcal{R}_\mathcal{E}$ indicated by blue dots. A set of initial conditions is selected from the border of the cut of $\mathcal{R}_\mathcal{E}$ (green dots), points marked with $*$, and as expected, their trajectories converges to the origin without leaving the safe region. Additionally, we take some points outside $\mathcal{R}_\mathcal{E}$: the ones marked in black lines still converge to the origin, despite not belonging to the estimate $\mathcal{R}_\mathcal{E}$; and those initial conditions in magenta lines generate divergent trajectories. For these cases, we choose θ_k as a sequence that leads the open-loop system to have unstable modes. We measured the average update rate for the trajectories in the border of the green region, finding 36.19%. Therefore, the proposed design allowed to reduce the updates in almost 2/3 of the samples with respect to the traditional (periodic) sample-data control, still ensuring regionally asymptotically stable trajectories.

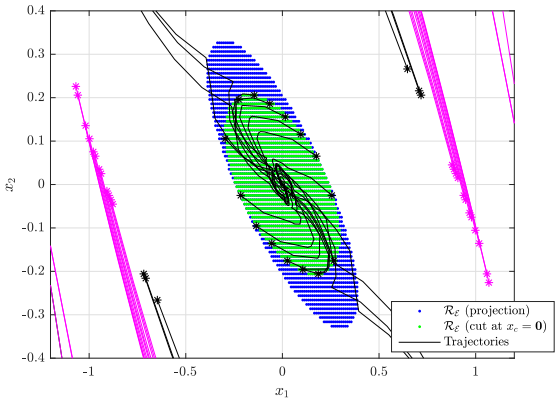

Figure 2: $\mathcal{R}_\mathcal{E}$ with event-triggering mechanism.

Note that, in this case, we are only concerned with reducing the update rate, which can result in a smaller attraction region as there is a trade-off between the attraction domain size and the transmission saving. In this sense, we can use the topic *iii)* of Remark 2 to design an LPV dynamic controller for a given ETM specified by the parameters σ and μ, whose choice benefits the size of such a region, thus increasing the update rates obtained with co-design.

5.2. Batch reactor inspired LPV model

In this example, we explore a fourth order LPV system to illustrate the application of our approach under different control objectives. Consider the

model (1)-(4) with matrices:

$$A_1 = \begin{bmatrix} 1.0171 & -0.0005 & 0.0341 & -0.0278 \\ -0.0026 & 0.9803 & 0.0203 & 0.0034 \\ 0.0052 & 0.0211 & 0.9875 & 0.0288 \\ 0.0002 & 0.0212 & 0.0066 & 0.9907 \end{bmatrix},\ B_1 = \begin{bmatrix} 0.0011 & -0.0001 \\ 0.0284 & 0.0016 \\ 0.0060 & -0.0145 \\ 0.0060 & -0.0001 \end{bmatrix},$$

$$A_2 = \begin{bmatrix} 0.9969 & -0.0015 & 0.0319 & -0.0278 \\ -0.0032 & 0.9773 & -0.0203 & 0.0034 \\ 0.0052 & 0.0211 & 0.9475 & 0.0288 \\ 0.0002 & 0.0210 & 0.0066 & 0.9887 \end{bmatrix},\ B_2 = \begin{bmatrix} -0.0011 & -0.0005 \\ 0.0278 & -0.0016 \\ 0.0060 & -0.0165 \\ 0.0060 & -0.0001 \end{bmatrix},$$

$$C = \begin{bmatrix} 1 & 0 & 1 & -1 \\ 0 & 1 & 0 & 0 \end{bmatrix}. \tag{41}$$

Note that the pair (A, B) with $A = (A_1 + A_2)/2$ and $B = (B_1 + B_2)/2$ corresponds to the unstable batch reactor discretized with sampling time $T_s = 0.005$ seconds investigated in [44]. Here, we have adapted such a model to represent it as an LPV one.

First, we consider a linear case, i.e., we assume actuators without saturation limits. Next, we take the saturation limits and provide designs including update rate and optimal cost minimizations.

5.2.1. Linear case with update rate minimization

We performed the co-design of the dynamic controller and the ETM parameters for the considered system without actuator saturation, and compared our results with those obtained by the approach proposed in [17], where a state-feedback controller is designed.

Thus, to minimize the update rate of the output signal, we use the optimization procedure $\mathcal{O}_1$ given in (26) with conditions of Theorem 2 and the changes mentioned in Remark 1 to disregard saturation. We got the following ETM matrices

$$Q_e = \begin{bmatrix} 7.2061 & 0.4851 \\ 0.4851 & 4.0287 \end{bmatrix},\ Q_y = \begin{bmatrix} 0.7836 & -0.1165 \\ -0.1165 & 0.8615 \end{bmatrix},\ Q_u = \begin{bmatrix} 1.2100 & 0.2905 \\ 0.2905 & 0.2032 \end{bmatrix}.$$

Then, we simulate the closed-loop system response assuming the initial condition $\xi(0) = \begin{bmatrix} -0.2430 & -0.2178 & -0.4239 & -0.2182 & \mathbf{0}_{1,4} \end{bmatrix}^\top$ and the parameter-varying $\theta_k = \cos(0.01\pi k)$. Figure 3 shows the four states (top), the two control inputs (middle), and the inter-event intervals of the ETM (bottom).

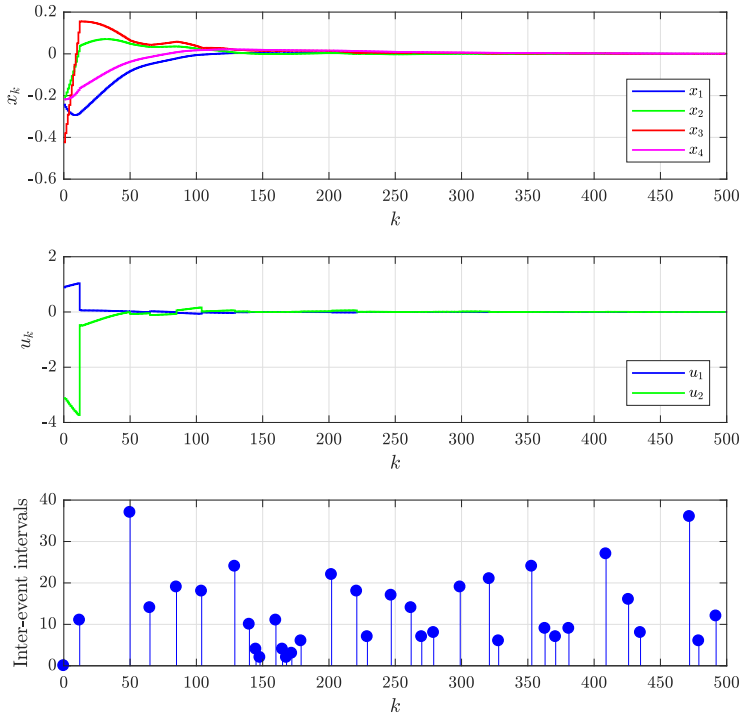

Figure 3: The closed-loop system response for $\theta_k = \cos(0.01\pi k)$ and $\xi(0) = \begin{bmatrix} -0.2430 & -0.2178 & -0.4239 & -0.2182 & \mathbf{0}_{1,4} \end{bmatrix}^\top$.

It is possible to see that the closed-loop system is asymptotically stable with 35 output updates on the simulation time-interval, which corresponds to an update rate as lower as 7%. Because this is a linear case, the initial condition can be as bigger as possible and there is no meaning to consider an estimate $\mathcal{R}_\mathcal{E}$.

In the sequel, we compare our approach with Theorem 1 given in [17], from which we got the ETM parameter $\sigma_x = 5.8042 \times 10^{-4}$ and the state-feedback

controller with gains

$$K_1 = \begin{bmatrix} 75.2256 & -10.3706 & 1.1084 & -145.6711 \\ 233.9475 & 18.5774 & 77.2793 & -221.0097 \end{bmatrix},$$

$$K_2 = \begin{bmatrix} 94.8493 & -5.9275 & 0.5269 & -134.6773 \\ 97.2623 & 13.4821 & 55.9525 & -108.5494 \end{bmatrix}.$$

The simulation of the closed-loop system response for the same time interval and initial conditions yielded an update rate of the control signal of 37.40%, which is almost 6 times bigger than ours, illustrating the better performance of our approach.

5.2.2. Saturating case with update rate minimization

In this case, we consider the saturation with $\bar{u} = \begin{bmatrix} 0.6 & 0.6 \end{bmatrix}^\top$. Applying the optimization procedure $\mathcal{O}_1$ given in (26) with conditions of Theorem 2, we did the co-design obtaining the ETM matrices:

$$Q_e = \begin{bmatrix} 8.0750 & 0.8996 \\ 0.8996 & 4.8406 \end{bmatrix},\ Q_y = \begin{bmatrix} 0.7215 & -0.1234 \\ -0.1234 & 0.8764 \end{bmatrix},\ Q_u = \begin{bmatrix} 1.2394 & 0.2767 \\ 0.2767 & 0.2034 \end{bmatrix}.$$

By using the same initial condition as in Section 5.2.1 (linear case) to simulate the closed-loop response, we can check that the trajectories do not converge to the origin, i.e. the system is unstable. As expected, in the presence of saturation, it is not possible to guarantee the asymptotic stability of the system for the entire state space, but only for a set of initial conditions. In fact, such an initial condition does not belong to the region of attraction of the origin for the system (41) in presence of input saturation.

Then, we consider $\xi(0) = \begin{bmatrix} -0.0540 & -0.0484 & -0.0942 & -0.0485 & \mathbf{0}_{1,4} \end{bmatrix}^\top$ as the initial condition, which belongs to the region $\mathcal{R}_\mathcal{E}$ defined in (12). The time-response was simulated, and Figure 4 shows the achieved results: state response (top), the control inputs (middle), and the inter-event interval of the ETM (bottom).

The asymptotic stability of the closed-loop is ensured despite the saturation of the second control signal (dashed green lines) during the interval $6 \leq k \leq 13$,

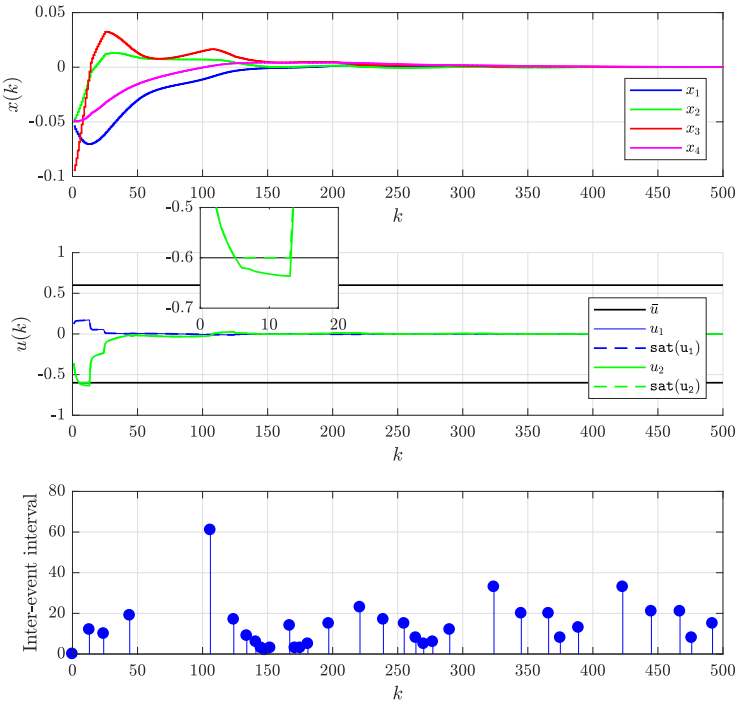

Figure 4: The closed-loop system response for $\theta_k = \cos(0.01\pi k)$ and $\xi(0) = \begin{bmatrix} -0.0540 & -0.0484 & -0.0942 & -0.0485 & \mathbf{0}_{1,4} \end{bmatrix}^\top$.

which is clear in the zoom presented in the middle plot of Figure 4. This test verifies an update rate of 6.60%.

5.3. LTI system under saturating actuators

Consider (1) as the discretized LTI model, with sampling time $T_s = 0.01$ s, of an inverted pendulum also investigated in [26, 27, 29]. The system matrices are given by

$$A = \begin{bmatrix} 1.0018 & 0.01 \\ 0.36 & 1.0018 \end{bmatrix}, \; B = \begin{bmatrix} -0.001 \\ -0.184 \end{bmatrix}, \; C = \begin{bmatrix} 1 & 0 \\ 0 & 1 \end{bmatrix}, \tag{42}$$

and the symmetric saturation limit is $\bar{u} = 1$. In this example, we study both the co-design and the emulation and compare the achievements of our approach with the finds in [26, 27, 29] where state feedback controller and input saturation is

considered. [27] addresses the emulation case, with a given ETM and the design of the controller. The co-design is proposed in [26, 29], and a dynamic state stabilizing controller is suggested in [26].

Considering the co-design approach provided by Theorem 2, we combine the optimization procedures $\mathcal{O}_1$ and $\mathcal{O}_3$, and use the objective function given by $\mathtt{tr}(7.2P_0) + \mathtt{tr}(Q_e + 0.95\hat{Q}_y) + \mathtt{tr}(0.05\hat{Q}_u)$, where the weights were adjusted by trial and error. As a result, we got the obtained ETM matrices:

$$Q_e = \begin{bmatrix} 1.3048 & 0.3967 \\ 0.3967 & 0.1206 \end{bmatrix}, \; Q_y = \begin{bmatrix} 0.1051 & 0.0608 \\ 0.0608 & 0.1001 \end{bmatrix}, \; Q_u = 0.0064,$$

Table 5.3 provides the summary of the achievements of our co-design approach and those from [26, 27, 29]. The initial conditions are $x(0) = \begin{bmatrix} 0.2 & 0.8 \end{bmatrix}^\top$ and $x_c(0) = \begin{bmatrix} 0 & 0 \end{bmatrix}^\top$ and the simulations take 1001 samples. Theorem 2 allows to

Table 1: Comparison of the number of samplings.

Design method	number of updates
Theorem 1 in [29]	90
Theorem 3.2 in [27]	218
Theorem 3.1 in [26]	67
Theorem 4.1 in [26]	70
Theorem 2	56

reduce the number of updates between 16.42% and 74.3%.

Next, we perform comparisons with the literature by using the emulation approach provide by Theorem 1. We made two emulation designs, one using the controller from Theorem 2, and the one given in [26]. In both cases, we simulated the closed-loop system under the designed ETM with the same initial conditions and simulations time previously used.

Assuming the controller of [26], we run a combination of the optimization procedures $\mathcal{O}_1$ and $\mathcal{O}_3$, see Remark 3, and the objective function given by

$\mathtt{tr}(3.6P_0) + \mathtt{tr}(Q_e + 0.95\hat{Q}_y) + \mathtt{tr}(0.05\hat{Q}_u)$, where the weights were found by trial and error. The obtained ETM matrices are

$$Q_e = \begin{bmatrix} 0.4230 & 1.0236 \\ 1.0236 & 2.8028 \end{bmatrix},\ Q_y = \begin{bmatrix} 0.0537 & 0.0062 \\ 0.0062 & 0.0630 \end{bmatrix},\ Q_u = 0.0058.$$

This emulation design achieves 62 updates, which is a better than the performance verified with [26, Theorem 4.1], reducing its updates in 11.43%.

By using the controller obtained by Theorem 2, we run the optimization procedure $\mathcal{O}_1$ with Theorem 1 adding a requirement: the cut of $\mathcal{R}_{\mathcal{E}}$ achieved in the co-design test must be guaranteed on plane x_k, ensuring that it remains with the same region of admissible initial conditions for the system. The following ETM matrices were obtained:

$$Q_e = \begin{bmatrix} 2.2262 & 0.6768 \\ 0.6768 & 0.2058 \end{bmatrix},\ Q_y = \begin{bmatrix} 0.0511 & 0.0301 \\ 0.0301 & 0.0612 \end{bmatrix},\ Q_u = 0.0144,$$

For such case, we have found a number of samplings equal to 33. Therefore, we reduced the number of updates in 41.07% in relation to that obtained by the co-design (Theorem 2). Moreover, with respect to [26, 27, 29], there was a reduction even more important, between 50.75% and 86.24%.

6. Conclusion

We proposed a methodology to co-design a dynamic output-feedback controller and an event-triggering mechanism for discrete-time LPV systems under saturating input. The method, based on LMI conditions, ensures the regional asymptotic stability of the closed-loop system for initial conditions belonging to an estimated region of attraction. We formulate some optimization procedures that allow the designer to minimize the data transmission rate from the sensor to controller, to maximize the size of the stability region, or to minimize the upper-bound of a quadratic linear cost function. The effectiveness of our proposal is illustrated and compared with the literature thought numerical tests, pointing out the classical trade-off between the different criteria of optimization.

In order to expand the results proposed, we could study more relaxing online availability of the varying parameter and a more general parameter dependence, as for example polynomial nature. Such a direction should impose to consider other methods as those based on sum-of-squares.

Appendix A. Proof of Theorem 1

By supposing the feasibility of (18), multiply its left-hand side by $\theta_{k(i)}$, and sum it up for $i \in \mathcal{I}[1, N]$. After, replace $H(\theta_k)$ by $G(\theta_k)U$, use the fact that $[P(\theta_k) - U]^\top P^{-1}(\theta_k)[P(\theta_k) - U] \geq \mathbf{0}$ [45] to over-bound the block (1,1) by $U^\top P^{-1}(\theta_k)U$, and pre- and post-multiply the resulting inequality by $\texttt{diag}\{U^{-\top}, 1\}$, to obtain

$$\begin{bmatrix} P^{-1}(\theta_k) & \star \\ G(\theta_k)_{(\ell)} & \bar{u}^2_{(\ell)} \end{bmatrix} \geq \mathbf{0}. \tag{A.1}$$

Finally, apply Schur complement and pre- and post-multiply the resulting inequality by $\xi(k)^\top$ and $\xi(k)$, respectively, to obtain

$$-\xi(k)^\top P(\theta_k)^{-1}\xi(k) + \xi(k)^\top \mathbb{G}(\theta_k)^\top_{(\ell)}(\bar{u}^2_{(\ell)})^{-1}\mathbb{G}(\theta_k)_{(\ell)}\xi(k) \leq 0, \tag{A.2}$$

thus, ensuring that $\mathcal{R}_\mathcal{E} \subset \mathcal{S}(\bar{u})$, $\forall k \geq 0$, i.e. any trajectory of the closed-loop system starting in $\mathcal{R}_\mathcal{E}$ remains in $\mathcal{S}(\bar{u})$.

By supposing the feasibility of (17), multiply its left-hand side by $\theta_{k+1(r)}$, $\theta_{k(i)}$ and $\theta_{k(j)}$, and sum it up for $r, i \in \mathcal{I}[1, N]$ and $j \in \mathcal{I}[1, N]$. Then, replace $H(\theta_k)$ by $G(\theta_k)U$, use the fact that $[P(\theta_k)-U]^\top P^{-1}(\theta_k)[P(\theta_k)-U] \geq \mathbf{0}$ to over-bound the block (1,1) by $U^\top P^{-1}(\theta_k)U$, and pre- and post-multiply the resulting inequality by $\texttt{diag}\{U^{-\top}, \mathbf{I}_p, S^{-1}, \mathbf{I}_{2n}, \mathbf{I}_p, \mathbf{I}_m\}$ and its transpose, respectively, to

get

$$\begin{bmatrix} P(\theta_k) & \star & \star & \star & \star & \star \\ \mathbf{0} & Q_e & \star & \star & \star & \star \\ -S^{-1}(\mathbb{K}(\theta_k) - G(\theta_k)) & -S^{-1}D_c(\theta_k) & 2S^{-1} & \star & \star & \star \\ \mathbb{A}(\theta_k) & \mathbb{E}(\theta_k) & -\mathbb{B}(\theta_k) & P(\theta_{k+1}) & \star & \star \\ \mathbb{C} & \mathbf{0} & \mathbf{0} & \mathbf{0} & \hat{Q}_y & \star \\ \mathbb{K}(\theta_k) & D_c(\theta_k) & \mathbf{0} & \mathbf{0} & \mathbf{0} & \hat{Q}_u \end{bmatrix} > \mathbf{0}. \tag{A.3}$$

Next, apply Schur complement three times and pre- and post-multiply the resulting inequality by $\begin{bmatrix} \xi(k)^\top & e(k)^\top & \Psi(u(k))^\top \end{bmatrix}$ and its transpose, respectively. Finally, replace $\mathbb{A}(\theta_k)\xi(k) + \mathbb{E}(\theta_k)^\top e(k) - \mathbb{B}(\theta_k)\Psi(u(k))$ by $\xi(k+1)$, see (9), and $\xi(k+1)^\top P^{-1}(\theta_{k+1})\xi(k+1) - \xi(k)^\top P^{-1}(\theta_k)\xi(k)$ by $\Delta V(\xi(k))$, i.e. consider

$$\begin{aligned} \Delta V(\xi(k)) &= \xi(k+1)^\top P^{-1}(\theta_{k+1})\xi(k+1) - \xi(k)^\top P^{-1}(\theta_k)\xi(k) \\ &= \Big(\mathbb{A}(\theta_k)\xi(k) + \mathbb{E}(\theta_k)e(k) - \mathbb{B}(\theta_k)\Psi(u(k))\Big)^\top P^{-1}(\theta_{k+1}) \\ &\quad \times \Big(\mathbb{A}(\theta_k)\xi(k) + \mathbb{E}(\theta_k)e(k) - \mathbb{B}(\theta_k)\Psi(u(k))\Big) - \xi(k)^\top P^{-1}(\theta_k)\xi(k) \end{aligned}$$

and denote $S^{-1} = M$, $\hat{Q}_y^{-1} = Q_y$ and $\hat{Q}_u^{-1} = Q_u$, to obtain

$$\begin{aligned} \Delta V(\xi(k)) - 2\Psi(u(k))^\top M(\Psi(u(k)) - (\mathbb{K}(\theta_k) - G(\theta_k))\xi(k) - D_c(\theta_k)e(k)) \\ < e(k)^\top Q_e e(k) - y(k)^\top Q_y y(k) - u(k)^\top Q_u u(k) \leq 0. \end{aligned} \tag{A.4}$$

Hence, the feasibility of (17) and (23) ensures the feasibility (A.2) and (A.4). Then one has both the positivity of the function given in (11) and the negativity of $\Delta V(\xi(k))$. Therefore, one can conclude that $\mathcal{R}_\mathcal{E}$ given in (12) is an estimation of the region of attraction of the origin for the closed-loop system.

Appendix B. Proof of Theorem 2

By supposing the feasibility of (23), from block (1,1), it follows that $\hat{U} + \hat{U}^\top > 0$, consequently, $\hat{U}$ is non-singular. Therefore, from (20), we have X and

Y non-singular and we can write $\hat{U}$ as

$$\hat{U} = \begin{bmatrix} Y^\top & F^\top \\ \mathbf{I}_n & X \end{bmatrix} = \begin{bmatrix} \mathbf{I}_n & Y^\top \\ \mathbf{0} & \mathbf{I}_n \end{bmatrix} \begin{bmatrix} \mathbf{0} & F^\top - Y^T X \\ \mathbf{I}_n & X \end{bmatrix}, \tag{B.1}$$

which allows us to conclude that $(F^\top - Y^\top X)$ is also non-singular. As a result, it is always possible to choose non-singular matrices W and Z, such that (21) is satisfied. This shows that the gains (25) are well-defined.

Moreover, by considering the matrices (19)-(22) and the change of variables $\hat{A}_{cij}$, $\hat{B}_{cij}$, $\hat{C}_{ci}$, $\hat{D}_{ci}$ and $\hat{E}_{ci}$ according to (25), pre- and post-multiply (23) by $\mathtt{diag}\{\Omega^{-\top}, \mathbf{I}_p, \Omega^{-\top}, \mathbf{I}_p, \mathbf{I}_m\}$ and its transpose, respectively, to get (17) and, likewise, pre- and post-multiply (24) by $\mathtt{diag}\{\Omega^{-\top}, 1\}$ and its transpose, respectively, to get (18). Thus, from Theorem 1, these two equivalences allow to conclude the proof.

References

[1] W. Heemels, K. H. Johansson, P. Tabuada, An introduction to event-triggered and self-triggered control, in: 2012 IEEE 51st IEEE Conference on Decision and Control (CDC), IEEE, 2012, pp. 3270–3285.

[2] A. Eqtami, D. V. Dimarogonas, K. J. Kyriakopoulos, Event-triggered control for discrete-time systems, in: Proceedings of the 2010 american control conference, IEEE, 2010, pp. 4719–4724.

[3] C. Peng, T. C. Yang, Event-triggered communication and $\mathcal{H}_\infty$control co-design for networked control systems, Automatica 49 (5) (2013) 1326–1332.

[4] S. Li, D. Sauter, B. Xu, Co-design of event-triggered $\mathcal{H}_\infty$ control for discrete-time linear parameter-varying systems with network-induced delays, Journal of the Franklin Institute 352 (5) (2015) 1867–1892.

[5] S. Tarbouriech, A. Seuret, J. M. Gomes da Silva Jr, D. Sbarbaro, Observer-based event-triggered control co-design for linear systems, IET Control Theory & Applications 10 (18) (2016) 2466–2473.

[6] J. Lunze, D. Lehmann, A state-feedback approach to event-based control, Automatica 46 (1) (2010) 211–215.

[7] W. Heemels, M. Donkers, A. Teel, Periodic event-triggered control for linear systems, IEEE Transactions on Automatic Control 58 (4) (2012) 847–861.

[8] W. Wu, S. Reimann, D. Görges, S. Liu, Suboptimal event-triggered control for time-delayed linear systems, IEEE Transactions on Automatic Control 60 (5) (2014) 1386–1391.

[9] X.-M. Zhang, Q.-L. Han, Event-triggered dynamic output feedback control for networked control systems, IET Control Theory & Applications 8 (4) (2014) 226–234.

[10] M. Abdelrahim, R. Postoyan, J. Daafouz, D. Nešić, Stabilization of nonlinear systems using event-triggered output feedback controllers, IEEE transactions on automatic control 61 (9) (2015) 2682–2687.

[11] W. Wu, S. Reimann, D. Görges, S. Liu, Event-triggered control for discrete-time linear systems subject to bounded disturbance, International Journal of Robust and Nonlinear Control 26 (9) (2016) 1902–1918.

[12] B. A. Khashooei, D. J. Antunes, W. Heemels, Output-based event-triggered control with performance guarantees, IEEE Transactions on Automatic Control 62 (7) (2017) 3646–3652.

[13] Y. Shen, F. Li, D. Zhang, Y.-W. Wang, Y. Liu, Event-triggered output feedback $\mathcal{H}_\infty$ control for networked control systems, International Journal of Robust and Nonlinear Control 29 (1) (2019) 166–179.

[14] C. Briat, Linear Parameter-Varying and Time-Delay Systems: Analysis, Observation, Filtering & Control, Springer-Verlag Berlin Heidelberg, Berlin, 2014.

[15] J. Mohammadpour, C. W. Scherer, Control of linear parameter varying systems with applications, Springer, New York, 2012.

[16] S. Li, B. Xu, Event-triggered control for discrete-time uncertain linear parameter-varying systems, in: Proceedings of the 32nd Chinese Control Conference, IEEE, 2013, pp. 273–278.

[17] A. Golabi, N. Meskin, R. Tóth, J. Mohammadpour, T. Donkers, Event-triggered control for discrete-time linear parameter-varying systems, in: 2016 American Control Conference (ACC), IEEE, 2016, pp. 3680–3685.

[18] X. Xie, S. Li, B. Xu, Output-based event-triggered control for networked control systems: tradeoffs between resource utilisation and robustness, IET Control Theory & Applications 12 (15) (2018) 2138–2147.

[19] S. Tarbouriech, G. Garcia, J. M. Gomes da Silva Jr., I. Queinnec, Stability And Stabilization Of Linear Systems With Saturating Actuators, Springer, 2011.

[20] W. Ni, P. Zhao, X. Wang, J. Wang, Event-triggered control of linear systems with saturated inputs, Asian Journal of Control 17 (4) (2015) 1196–1208.

[21] G. A. Kiener, D. Lehmann, K. H. Johansson, Actuator saturation and anti-windup compensation in event-triggered control, Discrete event dynamic systems 24 (2) (2014) 173–197.

[22] A. Seuret, C. Prieur, S. Tarbouriech, L. Zaccarian, LQ-based event-triggered controller co-design for saturated linear systems, Automatica 74 (2016) 47–54.

[23] D. Liu, G.-H. Yang, Event-triggered control for linear systems with actuator saturation and disturbances, IET Control Theory & Applications 11 (9) (2017) 1351–1359.

[24] Z. Zuo, S. Guan, Y. Wang, H. Li, Dynamic event-triggered and self-triggered control for saturated systems with anti-windup compensation, Journal of the Franklin Institute 354 (17) (2017) 7624–7642.

[25] L. Li, W. Zou, S. Fei, Event-based dynamic output-feedback controller design for networked control systems with sensor and actuator saturations, Journal of the Franklin Institute 354 (11) (2017) 4331–4352.

[26] S. Ding, X. Xie, Y. Liu, Event-triggered static/dynamic feedback control for discrete-time linear systems, Information Sciences 524 (2020) 33–45.

[27] W. Wu, S. Reimann, S. Liu, Event-triggered control for linear systems subject to actuator saturation, IFAC Proceedings Volumes 47 (3) (2014) 9492–9497.

[28] Z. Zuo, Q. Li, H. Li, Y. Wang, Co-design of event-triggered control for discrete-time systems with actuator saturation, in: 2016 12th World Congress on Intelligent Control and Automation (WCICA), IEEE, 2016, pp. 170–175.

[29] L. Groff, L. Moreira, J. Gomes da Silva, Event-triggered control co-design for discrete-time systems subject to actuator saturation, in: 2016 IEEE Conference on Computer Aided Control System Design (CACSD), IEEE, 2016, pp. 1452–1457.

[30] Y. Ma, W. Wu, D. Görges, B. Cui, Event-triggered feedback control for discrete-time piecewise affine systems subject to input saturation, Nonlinear Dynamics 95 (3) (2019) 2353–2365.

[31] M. F. Braga, C. F. Morais, E. S. Tognetti, R. C. L. F. Oliveira, P. L. D. Peres, Discretization and discrete-time output feedback control of linear parameter varying continuous-time systems, in: 53rd IEEE Conference on Decision and Control, IEEE, 2014, pp. 4765–4771.

[32] R. Tóth, P. S. C. Heuberger, P. M. J. Van den Hof, Discretisation of linear parameter-varying state-space representations, IET control theory & applications 4 (10) (2010) 2082–2096.

[33] J. Gomes da Silva Jr, J. F. V.M. Moraes, A. Palmeira, Sampled-data lpv control: a looped functional approach, IFAC-PapersOnLine 48 (26) (2015) 19–24.

[34] A. Palmeira, J. Gomes da Silva Jr, J. V. Flores, Aperiodic sampled-data control for LPV systems under input saturation, IFAC-PapersOnLine 51 (26) (2018) 130–136.

[35] R. Tóth, F. Felici, P. Heuberger, P. Van den Hof, Crucial aspects of zero-order hold LPV state-space system discretization, IFAC Proceedings Volumes 41 (2) (2008) 4952–4957.

[36] Z. Emedi, A. Karimi, Fixed-structure LPV discrete-time controller design with induced $\updownarrow_2$-norm and $\mathcal{H}_2$ performance, International Journal of Control 89 (3) (2016) 494–505.

[37] V. Verdult, Nonlinear system identification: State-space approach, Ph.D. thesis, Faculty of Applied Physics,University of Twente, Enschede, The Netherlands (2002).

[38] V. Cerone, D. Piga, D. Regruto, R. Toth, Input-output LPV model identification with guaranteed quadratic stability, IFAC Proceedings Volumes 45 (16) (2012) 1767–1772.

[39] M. Donkers, W.P.M.H.Heemels, Output-based event-triggered control with guaranteed $\mathcal{L}_\infty$-gain and improved event-triggering, in: 49th IEEE Conference on Decision and Control (CDC), IEEE, 2010, pp. 3246–3251.

[40] C. de Souza, V. J. S. Leite, S. Tarbouriech, E. B. Castelan, Emulation-based dynamic output-feedback control of saturating discrete-time LPV systems, IEEE Control Systems Letters 5 (2021) 1549 – 1554.

[41] C. Scherer, P. Gahinet, M. Chilali, Multiobjective output-feedback control via LMI optimization, IEEE Transactions on Automatic Control 42 (7) (1997) 896–911.

[42] L. Groff, L. Moreira, J. Gomes da Silva, D. Sbarbaro, Observer-based event-triggered control: A discrete-time approach, in: 2016 American Control Conference (ACC), IEEE, 2016, pp. 4245–4250.

[43] C. de Souza, S. Tarbouriech, E. B. Castelan, V. J. S. Leite, Event-triggered dynamic output-feedback controller for discrete-time LPV systems with constraints, in: 24th International Symposium on Mathematical Theory of Networks and Systems, 2020, pp. 1–6, accepted.

[44] J. Xiong, J. Lam, Stabilization of networked control systems with a logic zoh, IEEE Transactions on Automatic Control 54 (2) (2009) 358–363.

[45] J. C. Geromel, R. H. Korogui, J. Bernussou, $\mathcal{H}_2$ and $\mathcal{H}_\infty$ robust output feedback control for continuous time polytopic systems, IET Control Theory & Applications 1 (5) (2007) 1541–1549.